

Diffusion Rates for Hydrogen on Pd(111) from Molecular Quantum Dynamics Calculations

Thiago Firmino and Roberto Marquardt*

Laboratoire de Chimie Quantique - Institut de Chimie - UMR 7177 CNRS/UdS

Université de Strasbourg

1, rue Blaise Pascal - BP 296/R8 - 67008 STRASBOURG CEDEX - France

Fabien Gatti

CTMM, Institut Charles Gerhardt - UMR 5253 CNRS/Université de Montpellier 2

34095 MONTPELLIER Cedex 05 - France

Wei Dong

Laboratoire de Chimie - UMR 5182 CNRS/Ecole Normale Supérieure de Lyon

46, Allée d'Italie, 69364 LYON Cedex 07 - France

(Dated: October 29, 2018)

Abstract

Diffusion rates are calculated on the basis of van Hove's formula for the dynamical structure factor (DSF) related to particle scattering at mobile adsorbates. The formula is evaluated quantum mechanically using eigenfunctions obtained from three dimensional realistic models for H/Pd(111) derived from first principle calculations. Results are compatible with experimental data for H/Ru(0001) and H/Pt(111), if one assumes that the total rate obtained from the DSF is the sum of a diffusion and a friction rate. A simple kinetic model to support this assumption is presented.

PACS numbers: 31.15.A-, 68.43.Jk, 68.43.Pq, 82.65.+r

Keywords: quantum diffusion, high dimensional quantum dynamics, heterogeneous catalysis

The diffusion of adsorbed particles is an important process intervening in heterogeneous catalysis. Yet, and despite the significant progress achieved in the past decades in the domain of surface science, our knowledge about such elementary steps in catalysis remain modest, both experimentally and theoretically. In the long time domain of milliseconds to seconds, scanning tunneling microscopy (STM) is capable of unraveling some of the details of this motion. For instance, Jewell *et. al.* report on quantum tunneling of isolated hydrogen atoms adsorbed on Cu(111) terraces, which are observed with STM and a spatial resolution of a few tenths of a nanometer [1]. These experiments, carried out at 5 K, show the potential technological application arising from the interaction between the mobile adsorbates leading to the formation of self-assembled clusters. However, the time resolution of these experiments does not allow us to follow the motion of the H atoms in real time, interpreted in these papers as arising from tunneling.

The motion of hydrogen atoms adsorbed on metal surfaces has been explored with picosecond time resolution in ^3He spin-echo experiments for H/Pt(111) [2] and H/Ru(0001) [3]. The primary result from these experiments is the intermediate scattering function (ISF) $I(\mathbf{q}, t)$, where \mathbf{q} is the wave vector related to the momentum transferred from the scattered ^3He atoms to the hydrogen atoms moving on the surface, and t is the time. In [3], experimental results obtained at several temperatures are rationalized by path-integral molecular dynamics calculations and quantum transition-state theory. From these analyses, the onset of the quantum tunneling regime was shown to occur at about 70 K, for the H/Ru(0001) system.

In the experimental work, the diffusion rate of the adsorbed particles is obtained from adjustments of time-dependent model exponential functions to the ISF and varies as a function of the momentum transferred to the adsorbed particles. The diffusion rate is related to quasi-elastic broadening of the dynamical structure factor (DSF) $S(\mathbf{q}, E)$, which is the temporal Fourier transform of the ISF. The ISF is the spatial Fourier transform of the pair correlation function proposed by L. van Hove [4], who also derived a general expression for the DSF in terms of the eigenvalues and eigenfunctions pertaining to the stationary vibrational states of the adsorbates. Alternatively, one might then determine the diffusion rate by inspection of the full width at half maximum (FWHM) of the DSF.

In the present work, we modify van Hove's formula as follows:

$$S(\mathbf{q}, E) = \sum_n P_n \sum_m \left| \sum_k^N \langle m | e^{i\mathbf{q}\mathbf{x}_k} | n \rangle \right|^2 L(E; (E_m - E_n), \Gamma_{nm}). \quad (1)$$

In this equation, $|n\rangle$ and $|m\rangle$ are vibrational eigenstates of the scattering centers at energies E_n and E_m ; P_n is the Boltzmann population distribution; \mathbf{x}_k is the position vector of the adsorbed particle k ($k = 1, \dots, N$). $L(E; E_0, \Gamma)$ is a normalized Lorentzian distribution peaked at E_0 and having a full width at half maximum (FWHM) Γ . In the original work of van Hove, this formula is given with a δ -function instead of the Lorentzian. The energy width Γ_{nm} can be related to the finite lifetimes of vibrational eigenstates. State $|n\rangle$ has the lifetime $\tau_n = h/(\pi\gamma_n)$, where γ_n is the width (FWHM) of the energy distribution of this state in the set of the true eigenstates of the full system including electronic motion or the motion of substrate atoms (phonons), and h is the Planck constant. The overall width (FWHM) arising from the combination of states $|n\rangle$ and $|m\rangle$ in Eq. (1) is $\Gamma_{nm} = \gamma_n + \gamma_m$.

In a recent work [5], we explored the prospect of Eq. (1) to calculate diffusion rates of the adsorbate from a purely quantum mechanical treatment of the dynamics. In the present work, we evaluate Eq. (1) using vibrational eigenvalues and eigenfunctions derived from a potential energy surface (PES) for the H/Pd(111) system [6] and a realistic model for the lifetimes of these states. In our three dimensional study, a single H atom is considered ($N = 1$, in Eq. (1)), mimicking a low coverage degree of the substrate. Experimental diffusion rates for this system have not been determined so far.

While vibrational eigenstates can be calculated rather straightforwardly, the determination of vibrational lifetimes is more involved and data are hardly found. Depopulation of vibrational eigenstates of adsorbates on metal substrates via formation of electron-hole pairs is expected to proceed on the picosecond time scale [7, 8], or even faster [9, 10]. This is about the time scale that can be reached with the ^3He spin-echo technique. In [10], lifetimes for the lowest excited vibrational states in the most stable H/Pd(111) adsorption sites have been calculated to be around 500 fs to 1.5 ps. The corresponding energy broadening range of 2.6 to 0.9 meV is up to three orders of magnitude larger than the broadening due to the diffusion of the adsorbates typically observed in the aforementioned ^3He spin-echo experiments. The relaxation rate due to the coupling to phonons is probably much smaller [11].

For converged numerical evaluations of Eq. (1), sums over many states are needed, typically 50 to 200. As we do not know the lifetimes for the entire set of states, we make an ad hoc model assumption based on the findings from [10]: vibrational ground states, i.e., node-less states at the stable adsorption sites, have a lifetime of 1 μs , i.e. a width of about 1.3 neV ; all vibrationally excited states have an intrinsic lifetime of about $\tau_1 = 527$ fs,

which corresponds to an intrinsic energy broadening $\gamma_i = h/(\pi\tau_i) = 2.5$ meV. In practice, the widths used in the Lorentzians of Eq. (1) will therefore be 2 neV, nearly 2.5 meV and 5 meV, if vibrational ground states occur doubly, simply or not at all in a term of the sum.

We use the Multiconfiguration Time Dependent Hartree (MCTDH) program suite [12, 13] to calculate vibrational eigenstates of the adsorbed particles. The analytical function derived in [6] was used to generate a natural potential representation [14, 15] with the aid of the “potfit” program contained in the MCTDH program package. Eigenfunctions were then calculated within the MCTDH program with the aid of the “block relaxation method” [16].

The system is represented in a set of non-Euclidean coordinates (see Figure 1 below) to fully exploit its periodicity. Note that the kinetic energy operator contains non-diagonal terms, when such coordinates are used [17]. For this three dimensional study, the analytical PES from [6] was first modified such as to describe a single hydrogen atom adsorbed on the palladium substrate. To achieve this, all hydrogen-hydrogen two-body terms, as well as the hydrogen-palladium-hydrogen three-body terms in the PES defined in [6] were zeroed, and the function definition was changed such as to depend on the coordinates of a single hydrogen atom. A graphical representation of a section of the PES is shown in Figure 1. More details on the calculations are given in the supplemental material.

This figure also shows the (2×2) surface cell underlying the present calculations. The stable adsorption sites denoted as “fcc” and “hcp” are clearly indicated. On this PES, the hcp site is about 190 hc cm^{-1} less stable than the fcc site and the barrier between the two sites is at about 1150 hc cm^{-1} above the fcc site. There are 4 fcc and 4 hcp sites per unit cell. The hcp/fcc occupation ratio is about 0.37 at room temperature, and we can therefore assume that the occupation of sites is approximately homogeneous, which makes the present study mimic a coverage degree of 12.5%, for the H/Pd(111) system.

Each site has a local C_{3v} symmetry, such that per site two vibrational modes parallel to the substrate and one mode perpendicular to it can be expected. Per site type there will hence be 4 vibrational ground states, and 12 vibrationally excited states, namely 8 states of parallel modes and 4 states of perpendicular modes, all arranged in levels of quasi-isoenergetic states. Tunneling may split these levels. The present calculations yield that the ground state levels at both the “fcc” and “hcp” sites remain degenerate. However, the vibrationally excited levels split into two blocks for each type of mode. The splitting could in principle be observed by high resolution spectroscopy. Table I summarizes expected

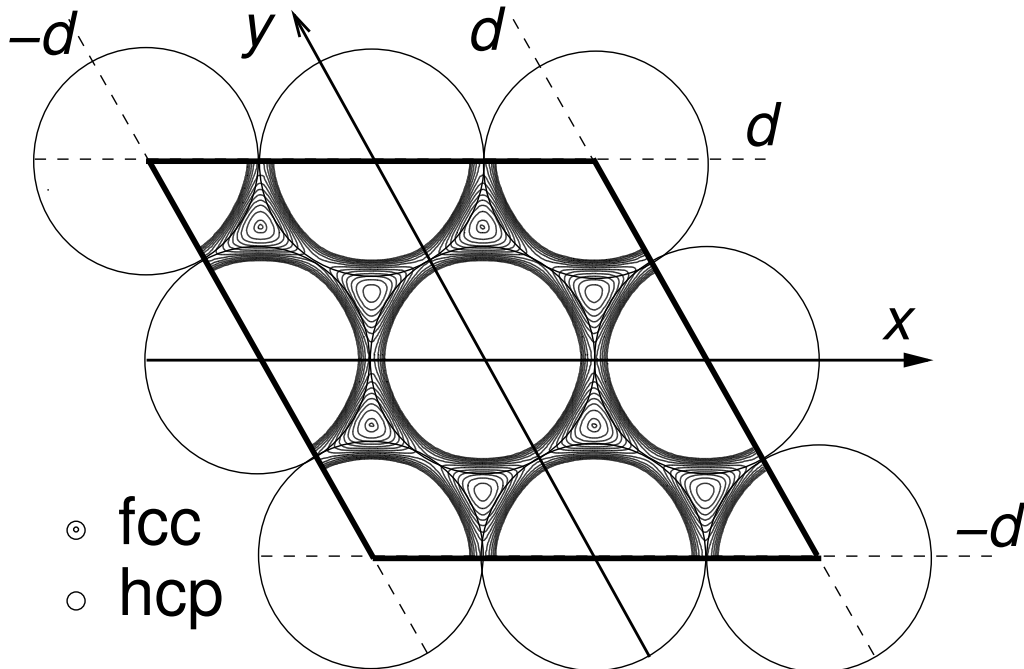


FIG. 1. Scheme of the (2×2) surface cell used to characterize the H/Pd(111) system. x and y are the skewed coordinates used in the dynamics. Palladium atoms are indicated by the large spheres of diameter d ($d = 275.114$ pm is the Pd-Pd bulk distance on the PES from [6]). A section of the PES for atomic hydrogen at $z = 90$ pm is superimposed on the scheme. Contour lines are separated by 200 hc cm^{-1} , the contour line indicated at most stable fcc site is 50 hc cm^{-1} (with a dot at the center), the highest, outermost lines shown are at 2650 hc cm^{-1} ; lines around hcp sites are at 250 hc cm^{-1} .

transitions, assuming that they occur vertically on top of each adsorption site.

Column “this work” in Table I reports four sets of vertical transitions for each mode, two sets of transitions per site type. These sets arise from the tunneling splitting of degenerate vibrationally excited levels and remaining degeneracies are indicated by the numbers in parentheses. In refs [17] and [18], only one value is reported per transition. The present results for vibrational wavenumbers are comparable to the previously reported values. Table I reports only the fundamental transitions. We note here that the calculated overtone spectrum indicates the presence of strong anharmonic resonances, which will have an important

TABLE I. Wavenumbers of the fundamental transitions for H/Pd(111) in cm^{-1} .

modes	site	theory		exp [18]	
		this work			
parallel	fcc	743.6 (5)	744.1 (3)	717.4	774.3
	hcp	726.8 (3)	730.8 (5)		
perpendicular	fcc	1047.6 (1)	1058.6 (3)	922.4	1016.3
	hcp	1000.2 (3)	1010.8 (1)		

influence on the short time diffusion dynamics. These results will be published elsewhere.

Vibrational states like those of the H/Pd(111) system in a (2×2) surface cell can be cast into a coarse grained level structure. Levels can be identified by the vibrational quantum number related to a specific adsorption site, while nearly degenerate states within a level compose a dense structure of states. Similar level structures arise for larger surface cells. Consequently, the DSF can be decomposed into a sum $S(\mathbf{q}, E) = \sum_l S_l(\mathbf{q}, E)$, where $l = 1, 2, \dots$ denotes a vibrational level.

Evaluation of Eq. (1) with the eigenvalues and widths discussed above yields a very narrowly peaked function at $E = 0$, the width of which is 2 neV. This width corresponds to the model lifetime assumed in this work for the vibrational ground states. It depends only very feebly on \mathbf{q} . Note that, as the Lorentzians in Eq. (1) are energy normalized, the form of the DSF at $E \sim 0$ is dominated by the contributions from the level of ground states. It is reasonable to omit these contributions, as they do apparently not influence the DSF further; in particular, they do not lead to any diffusion broadening. In the following, we consider therefore the differential DSF

$$\Delta S(\mathbf{q}, E) = S(\mathbf{q}, E) - S_1(\mathbf{q}, E), \quad (2)$$

where $S_1(\mathbf{q}, E) \approx S_1(0, E)$ is the contribution to $S(\mathbf{q}, E)$ from the level of ground states. Figure 2 shows the normalized function $\Delta S(\mathbf{q}, E)/\Delta S(\mathbf{q}, 0)$ along the $\langle 11\bar{2}0 \rangle$ direction, for $T = 250$ K. For this direction, the scalar product $\mathbf{q} \cdot \mathbf{x}$ is evaluated by the expression $q(x - y/2)$, because of the non-orthogonality of the x and y axes.

At a first sight, the FWHM of this function depends again little on the transferred momentum wave number q . It is roughly given by $\Gamma_i = 5$ meV, as expected for the intrinsic energy width adopted for the excited vibrational states in the model calculations of the

present work. When magnified one sees, however, a neat progression of lines (insert in Figure 2). Clearly, it is the *differential width* $\Delta\Gamma = \Gamma - \Gamma_i$ that varies with q .

To show this variation in detail, we plot in Figure 3 the rate

$$\alpha_d = \pi \Delta\Gamma/h \quad (3)$$

$\approx 0.759634 \text{ ps}^{-1} \times \Delta\Gamma/\text{meV}$. The figure shows α_d along the two crystallographic directions $\langle 11\bar{2}0 \rangle$ and $\langle 1\bar{1}00 \rangle$ and several temperatures. Note that, for the latter crystallographic direction, the scalar product $\mathbf{q} \cdot \mathbf{x}$ is evaluated by the expression $q \sqrt{3}/2 (x - y)$.

The solid line in the figure on the left hand side corresponds to the variation obtained in Figure 2. To our knowledge, there is currently no comparable experimental result for the H/Pd(111) system. We may compare the present theoretical result, however, with results obtained in the ^3He Spin Echo experiments for the diffusion rates for the H/Ru(0001) [3, figure 1 c] and H/Pt(111) [2, figure 2] systems, at similar coverage degrees (~ 0.1 monolayer). We see that α_d reproduces well the general behavior of the experimentally obtained function; the variation range for α_d is about a factor 10 larger than that observed for H/Ru(0001), and of the same order as that for H/Pt(111) ($\langle 11\bar{2}0 \rangle$ direction). Despite the remaining quantitative differences, the comparison with the experimental results leads us to

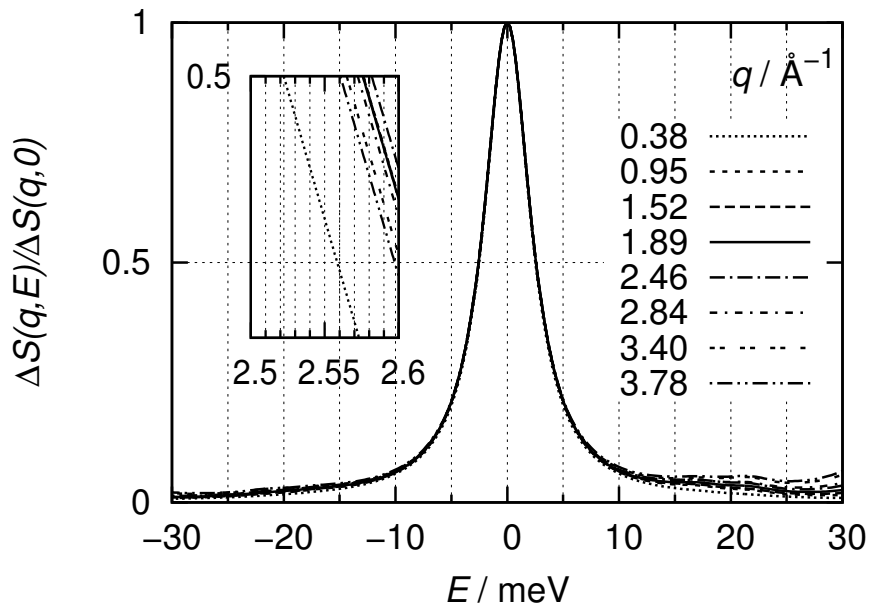


FIG. 2. $\Delta S(q, E)/\Delta S(q, 0)$ as a function of E and q for atomic hydrogen on Pd(111). The inset is a magnification of the function (right wing). Lines are cubic spline interpolations.

call α_d the *diffusion rate*.

As an additional support for our interpretation of α_d as being the same diffusion rate as that determined in the ^3He Spin Echo experiments, Figure 4 shows an Arrhenius plot of the temperature dependence of α_d . This result is again quite similar to that obtained for H/Pt(111) [2, figure 3] and predicts that also the diffusion rate of hydrogen on palladium should have a non classical behavior.

We can explain that the differential width corresponds indeed to the diffusion rate. We have developed a theory for the calculation of the ISF from the vibrational structure of the adsorbates. Variations of the differential width are shown to be related with the vibrational structure of the adsorbates and with the overlap of individual lines as a function of the intrinsic width. A detailed account of the theory as well as a discussion of the quantum effects will be presented elsewhere. In the present paper we develop a simple kinetic model to rationalize the variability of the differential width as a function of the transferred momentum. Starting from the kinetic model for jump diffusion [19], we extend it to include relaxation by friction. We write the equation of motion for the probability of finding a particle at position

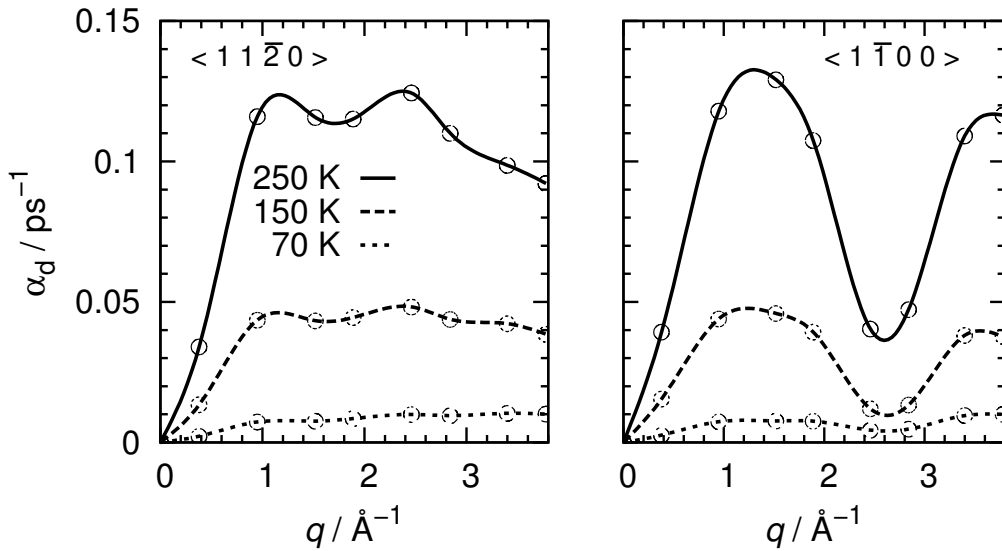


FIG. 3. Diffusion rate (see text) along two crystallographic directions and several temperatures, as indicated. Lines are cubic spline interpolations.

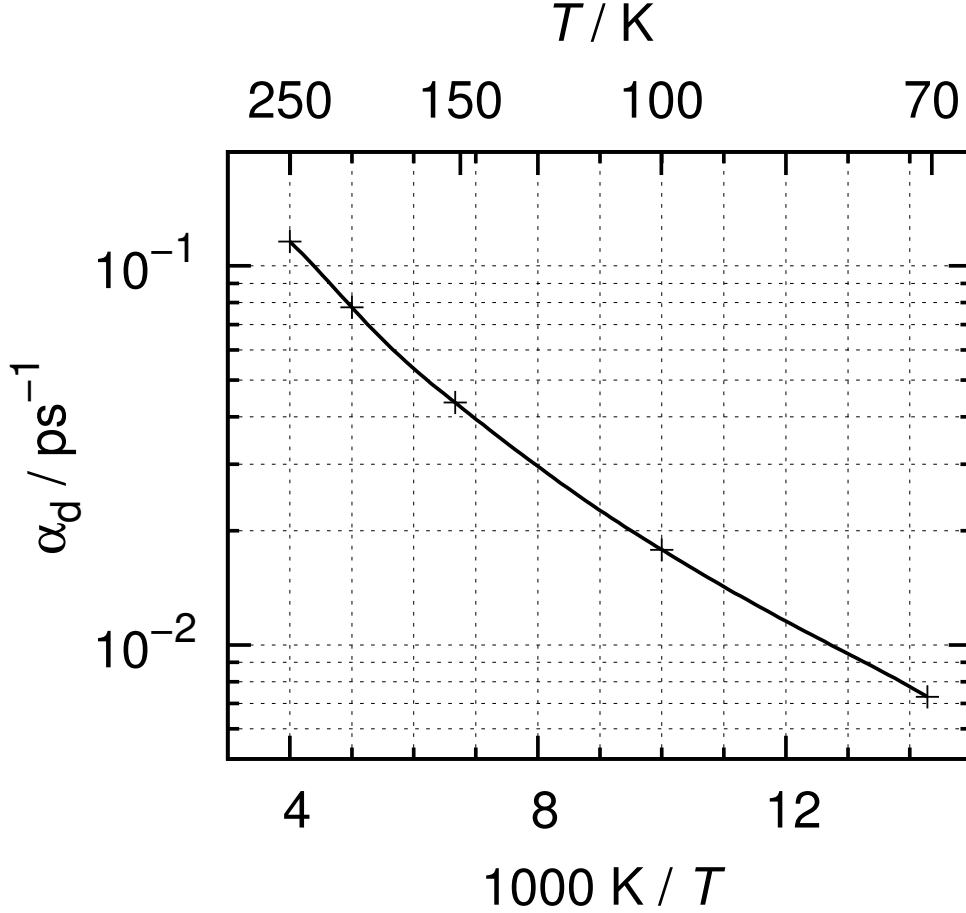


FIG. 4. Arrhenius plot of the temperature dependence of α_d ; $\langle 11\bar{2}0 \rangle$ crystallographic direction and $q = 0.95 \text{ \AA}^{-1}$.

\mathbf{x} at time t as [20]

$$\frac{\partial P(\mathbf{x}, t)}{\partial t} = \frac{1}{\tau} \left(\sum_k (P(\mathbf{x} + \mathbf{y}_k, t) - P(\mathbf{x}, t)) \right) - \frac{1}{\tau_i} P(\mathbf{x}, t). \quad (4)$$

The first part of the right hand side involves summation over lattice vectors and corresponds to the original jump diffusion model; it leads to the well known classical exponential decay for the ISF, if one assumes that the $P(\mathbf{x}, t)$ equals $G_s(\mathbf{x}, t)$, the self-part of the pair correlation function. This decay can even be a more involved model expression of several exponential functions [20], or it can be replaced by an even more complicated function that one might determine from quantum dynamics. The second part on the right hand side of Eq. (4) leads to a simple exponential decay of the ISF. Now, if the first part leads to a quasi-exponential decay, as it apparently does, the total decay rate is then given as the sum of the decay rates of the two parts. Consequently, it is the difference of the total width and the width due

to relaxation by friction that depends strongly on the momentum transfer, and which is generally related to the diffusion motion.

We have also evaluated Eq. (1) for the six dimensional system $\text{H}_2/\text{Pd}(111)$, using the same assumptions regarding the intrinsic life times of vibrationally excited states. Preliminary results indicate that the form of α_d changes significantly and that comparison with the experimental results for hydrogen on platinum becomes more favorably. When these results are confirmed, and experimental results for the diffusion rate of hydrogen on palladium are available, we should have an additional source of information regarding the structure of adsorbed hydrogen on palladium. The computational method described in this paper can be extended to calculations of the diffusion dynamics on other transition metal atoms, which can then be discussed in relation with the findings from ref. [1].

Finally, a comment about the lifetimes of vibrationally excited states is appropriate. In the simplified treatment of the present calculations, a generic realistic value for the life time of excited vibrational states has been adopted. Relevant life times from ref. [10] differ only little from the adopted value and if these are used instead of the generic one for the few states for which they are known, results change insignificantly. However, if the values for intrinsic life times change by a factor of 2 or more, so does the calculated diffusion rate [5]. Therefore, the calculation method for the diffusion rates of adsorbates developed in the present work is, in combination with their experimental determination, a new interesting tool to also determine relaxation rates of adsorbates.

This work was carried out within a research program from the *Agence Nationale de la Recherche* (project ANR 2010 BLAN 720 1). We thank ANR for the generous financial support, as well as CNRS and Université de Strasbourg.

* corresponding author: roberto.marquardt@unistra.fr

- [1] A. D. Jewell, G. Peng, M. F. G. Mattera, E. A. Lewis, C. J. Murphy, G. Kyriakou, M. Mavrikakis, and E. C. H. Sykes, *ACS Nano* **6**, 10115 (2012).
- [2] A. P. Jardine, E. Y. M. Lee, D. J. Ward, G. Alexandrowicz, H. Hedgeland, W. Allison, J. Ellis, and E. Pollak, *Phys. Rev. Lett.* **105**, 136101 (2010).
- [3] E. M. McIntosh, K. T. Wikfeldt, J. Ellis, A. Michaelides, and W. Allison, *J. Phys. Chem.*

- Letters **4**, 1565 (2013).
- [4] L. van Hove, Phys. Rev. **95**, 249 (1954).
- [5] T. Firmino, R. Marquardt, F. Gatti, D. Zanuttini, and W. Dong, in *Frontiers in Quantum Methods and Applications in Chemistry and Physics: Selected and Edited Proceedings of QSCP-XVIII (Paraty, Brazil, December 2013)*, Progress in Theoretical Chemistry and Physics, edited by M. A. C. Nascimento (Springer, Berlin, 2014), submitted.
- [6] Y. Xiao, W. Dong, and H. F. Busnengo, J. Chem. Phys. **132**, 014704 (2010).
- [7] M. Morin, N. J. Levinos, and A. L. Harris, J. Chem. Phys. **96**, 3950 (1992).
- [8] C. Frischkorn and M. Wolf, Chem. Rev. **106**, 4206 (2006).
- [9] T. Vazhappilly, S. Beyvers, T. Klamroth, M. Luppi, and P. Saalfrank, Chem. Phys. **338**, 299 (2007).
- [10] J. C. Tremblay, J. Chem. Phys. **138**, 244106 (2013).
- [11] M. Head-Gordon and J. C. Tully, J. Chem. Phys. **96**, 3939 (1992).
- [12] G. A. Worth, M. H. Beck, A. Jäckle, and H.-D. Meyer, The MCTDH Package, Version 8.2, (2000). H.-D. Meyer, Version 8.3 (2002), Version 8.4 (2007), Revision 8 (2012). See <http://mctdh.uni-hd.de/>.
- [13] M. H. Beck, A. Jäckle, G. A. Worth, and H.-D. Meyer, Phys. Rep. **324**, 1 (2000).
- [14] A. Jäckle and H.-D. Meyer, J. Chem. Phys. **104**, 7974 (1996).
- [15] A. Jäckle and H.-D. Meyer, J. Chem. Phys. **109**, 3772 (1998).
- [16] L. J. Doriol, F. Gatti, C. Iung, and H.-D. Meyer, J. Chem. Phys. **129**, 224109 (2008).
- [17] J. C. Tremblay and P. Saalfrank, J. Chem. Phys. **131**, 084716 (2009).
- [18] H. Conrad, M. Kordesch, R. Scala, and W. Stenzel, Journal of Electron Spectroscopy and Related Phenomena **38**, 289 (1986).
- [19] Chudley, C. T. and Elliot, R. J., Proc. Phys. Soc. **77**, 353 (1961).
- [20] F. E. Tuddenham, H. Hedgeland, A. P. Jardine, B. A. Lechner, B. Hinch, and W. Allison, Surface Science **604**, 1459 (2010).